

## Turing model for the patterns of lady beetles

S. S. Liaw,<sup>1</sup> C. C. Yang,<sup>2</sup> R. T. Liu,<sup>1</sup> and J. T. Hong<sup>1</sup>

<sup>1</sup>*Department of Physics, National Chung-Hsing University, Taichung 402, Taiwan*

<sup>2</sup>*Department of Physics, National Changhua Normal University, Changhua, Taiwan*

(Received 20 April 2001; published 21 September 2001)

We simulate the patterns on the hard wings of lady beetles using a reaction-diffusion equation based on the Turing model. A part of a spherical surface is used to approximate the geometry of the hard wings. Various patterns common to lady beetles in Taiwan can be produced on this curved surface by adjusting the parameters of the model.

DOI: 10.1103/PhysRevE.64.041909

PACS number(s): 87.10.+e, 87.17.Aa, 47.54.+r

### I. INTRODUCTION

In 1952 Turing proposed a general model for generating biological patterns [1]. The model was realized in some definite forms and has been used successfully to produce patterns in various biological cases such as seashells, fish, zebras, leopards, giraffes, etc. [2]. The formation of patterns and their stabilities in these kinds of reaction-diffusion model are well studied and understood in the general sense [3,4]. However, a specific pattern cannot be predicted. This is because there are several parameters that can be adjusted to produce all kinds of possibilities in any of these models.

In most of these systems, calculations are done on a flat surface. That is, the reaction-diffusion equations in the model are solved on a surface of zero curvature. The curvature of the geometry of the system is not taken into consideration. Recently, Varea, Aragon, and Barrio solved a Turing model on a spherical surface [5]. In their work they produced symmetric spot patterns on a sphere, which can be considered as a first step toward simulating the patterns of some microscopic organisms such as radiolarians and viruses. In this work, we consider a different type of Turing model on a spherical surface. A portion of a spherical surface is used to approximate the shape of the hard wings of lady beetles. We demonstrate that the model we use can yield patterns similar to those of the lady beetles.

### II. PATTERNS OF LADY BEETLES

Lady beetles (coccinellids) are familiar to people because of their beauty and interesting behavior. They are of a size about 0.8 to 1.8 cm. They have pleasing rounded forms and usually have bright, contrasting red and black colors. They like to walk along a stem all the way up and fly away from the top (Fig. 1). In case of danger, they will lie on their backs motionlessly for a long time, then suddenly turn onto their feet and fly away. The beetles have a pair of thickened wings, the elytra, which protect the hind wings and soft abdomen underneath. The elytra of the adult emerging from the pupa are soft, light in color, and without pattern. It takes minutes, hours, or in some cases days for the pattern to appear on the elytra.

There are over 4500 species of lady beetles on earth. The conspicuous pattern on the elytra can be easily identified for any particular species. Except for a few species, lady beetles have definite, recognizable patterns. That is, these patterns are stable with respect to evolution. Spots pattern are most common. Some have stripes or a combination of spots and stripes. Patterns on the elytra are always symmetric. That is, the positions, sizes, and colors of spots and stripes are identical on the two hard wings.

### III. THE MODEL

The generic form of the Turing model consists of two types of morphogen, say  $u$  and  $v$ , interacting with each other while diffusing on a surface. It can be written as

$$\frac{\partial u}{\partial t} = D_u \nabla^2 u + f(u, v), \quad (1)$$

$$\frac{\partial v}{\partial t} = D_v \nabla^2 v + g(u, v),$$

where  $D_u$  and  $D_v$  are the diffusion coefficients of the morphogens  $u$  and  $v$ , respectively. Although the actual interac-

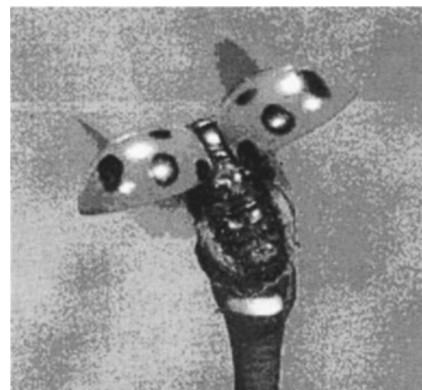


FIG. 1. A seven-star lady beetle on the top of a stem is ready for takeoff.

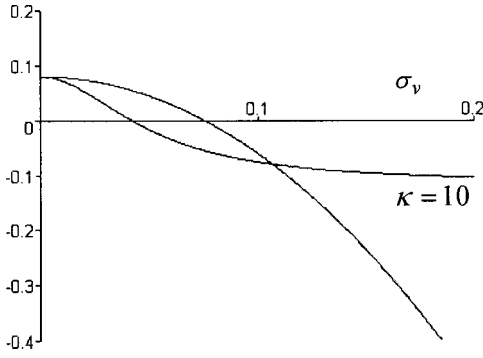


FIG. 2. For the model given by Eqs. (2) and (4), the constant production term  $\sigma_v$  has a minimal positive value in order to generate a pattern according to the requirement of Eq. (3a). The plot is the value of  $f_u + g_v$  as a function of  $\sigma_v$  for two different values of  $\kappa$ ,  $\kappa=0$  and 10.

tion between  $u$  and  $v$  is unknown, there are a few models with explicit forms for  $f(u, v)$  and  $g(u, v)$  that can generate large varieties of biological patterns. We take the model introduced by Gierer and Meinhardt used for activator-substrate systems [6]. Explicitly, it is

$$\begin{aligned} f(u, v) &= \rho_u \frac{u^2 v}{1 + \kappa u^2} - \mu_u u, \\ g(u, v) &= -\rho_v \frac{u^2 v}{1 + \kappa u^2} + \sigma_v, \end{aligned} \quad (2)$$

where  $\rho_u$ ,  $\rho_v$ ,  $\mu_u$ ,  $\sigma_v$ , and  $\kappa$  are non-negative constants. That is, we assume that  $u$  and  $v$  interact effectively according to the form  $u^2 v$ , the interaction saturates when  $u$  gets large, and the saturation constant  $\kappa$  is nonzero.  $v$  is consumed at the rate  $\rho_v$  in activating the increase of  $u$  at the rate  $\rho_u$ .  $u$  is removed at the rate  $\mu_u$  proportional to the amount of  $u$ . There is also a constant production term  $\sigma_v$  for  $v$ . With zero-flux boundary conditions, i.e.,  $\hat{\mathbf{n}} \cdot \nabla u = 0$ ,  $\hat{\mathbf{n}} \cdot \nabla v = 0$  on the boundary, the general conditions for the generation of spatial patterns are given by [4]

$$f_u + g_v < 0, \quad (3a)$$

$$D_v f_u + D_u g_v > 0, \quad (3b)$$

$$f_u g_v - f_v g_u > 0, \quad (3c)$$

$$(D_v f_u - D_u g_v)^2 + 4 D_u D_v f_v g_u > 0, \quad (3d)$$

$$D_u = 0.0005, \quad D_v = 50 D_u$$

$$D_u = 0.0005, \quad D_v = 100 D_u$$

$$D_u = 0.02, \quad D_v = 50 D_u$$

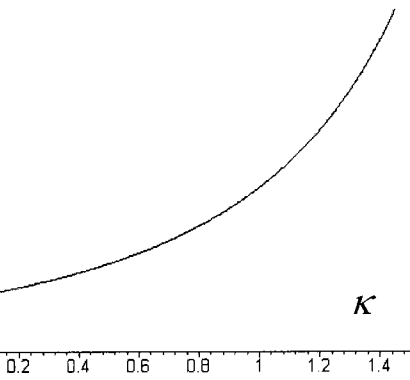
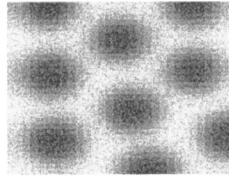
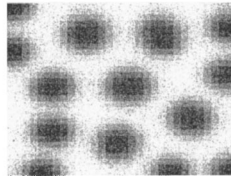
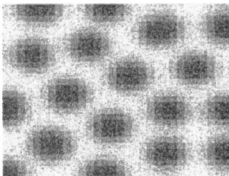


FIG. 3. According to the requirement of Eq. (3d), the threshold value of the ratio  $D_v/D_u$  is plotted as a function of  $\kappa$ . It can be seen from the plot that the diffusion constant for  $v$  has to be larger than that of  $u$  in order to generate patterns.

where the derivatives of  $f$  and  $g$  with respect to  $u$  and  $v$  (namely,  $f_u \equiv \partial f / \partial u$ , etc.) are evaluated at the steady state  $(u_0, v_0)$  such that  $f(u_0, v_0) = 0$ ,  $g(u_0, v_0) = 0$ . For example, in our calculation below, we fix the values of the parameters:

$$\rho_u = 0.18, \quad \rho_v = 0.36, \quad \mu_u = 0.08. \quad (4)$$

To satisfy Eq. (3a), a constant production rate of  $v$  must be present (see Fig. 2). The crucial condition for the appearance of patterns is that  $v$  must diffuse faster than  $u$  does, namely,  $D_v/D_u > 1$ . For example, choosing Eq. (4) and

$$\sigma_v = 0.1, \quad (5)$$

the threshold value of the ratio  $D_v/D_u$  as a function of  $\kappa$  is plotted in Fig. 3. Values of  $D_v/D_u$  below the curve cannot generate patterns. The minimal value of  $D_v/D_u$  is 7.8 when  $\kappa = 0$ .

When these conditions are satisfied, a spot pattern will appear when  $\kappa = 0$ . On increasing the ratio  $D_v/D_u$  or the values of  $D_u$  and  $D_v$ , fewer but larger spots appear (see Fig. 4). Turning on the saturation effect  $\kappa \neq 0$  leads to the formation of stripes (see Fig. 5).

#### IV. NUMERICAL CALCULATION

The geometry of the hard wings of lady beetles is a portion of a curved surface. The basic patterns on the curved surface are not different from those on a flat surface. However, the exact positions and shapes of the spots and stripes

FIG. 4. A square flat surface is used for demonstrating the general patterns of our model. Spot pattern is dominant when the saturation constant is zero,  $\kappa = 0$ . Increasing the ratio  $D_v/D_u$  or both values of  $D_u$  and  $D_v$ , we get fewer but larger spots. Constants for getting these patterns are chosen as follows:  $\rho_u = 0.01$ ,  $\rho_v = 0.02$ ,  $\mu_u = 0.01$ , and  $\sigma_v = 0.02$ .

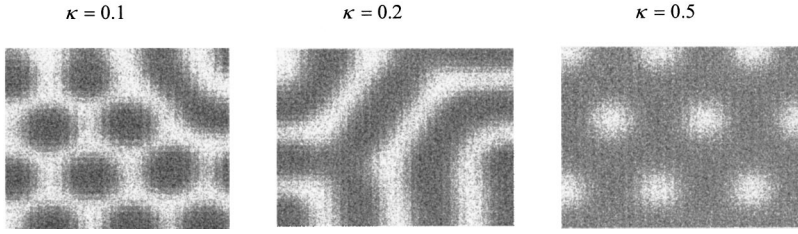


FIG. 5. When the saturation constant is not zero, a stripe pattern appears. At larger  $\kappa$ , the pattern is multiply connected. In this plot,  $D_u = 0.005$ ,  $D_v = 50D_u$ , and other constants are the same as in Fig. 4.

are strongly dependent on the curvature of the surface and the shape of the boundary [7]. We approximate the surface of the hard wings by a part of a sphere; the surface is defined by the area with spherical coordinates  $\theta_0 < \theta < \pi$ ,  $0 < \varphi < \pi$  (the radius of the spherical surface can be chosen to be 1 by adjusting the scale of all the equations) (see Fig. 6). To simulate the diffusion process, we use  $M \times N$  grids on the surface of a half hemisphere. That is, we discretize the distributions  $u(\theta, \varphi)$  and  $v(\theta, \varphi)$  as  $u(i, j)$  and  $v(i, j)$  evaluated at  $i = (m - \frac{1}{2})\pi/M$ ,  $m = i_0, \dots, M$ ,  $j = (n - \frac{1}{2})\pi/M$ ,  $n = j_0, \dots, N - j_0 + 1$ . We choose  $M = 48$ ,  $N = 48$ ,  $i_0 = 9$ , and  $j_0 = 1$  in some of our calculation and  $M = 72$ ,  $N = 72$ ,  $i_0 = 19$ , and  $j_0 > 1$  in others, as indicated in the figures. The evolutions of the distributions are calculated using the Euler method. That is, the value of  $u(i, j)$  at time  $t = (k + 1)\Delta t$  is given by

$$u_{k+1}(i, j) = u_k(i, j) + \Delta t * [D_u \nabla^2 u_k(i, j) + f(u_k(i, j), v_k(i, j))]. \quad (6)$$

The Laplace operator is approximated by the difference equation

$$\begin{aligned} \nabla^2 u_k(i, j) = & \frac{1}{(\Delta \theta)^2} [u_k(i+1, j) + u_k(i-1, j) - 2u_k(i, j)] \\ & + \frac{1}{\tan \theta} \frac{1}{2\Delta \theta} [u_k(i+1, j) - u_k(i-1, j)] \\ & + \frac{1}{\sin^2 \theta} \frac{1}{(\Delta \varphi)^2} [u_k(i, j+1) + u_k(i, j-1) \\ & - 2u_k(i, j)], \end{aligned} \quad (7)$$

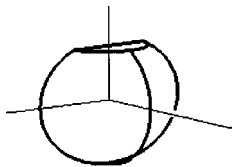
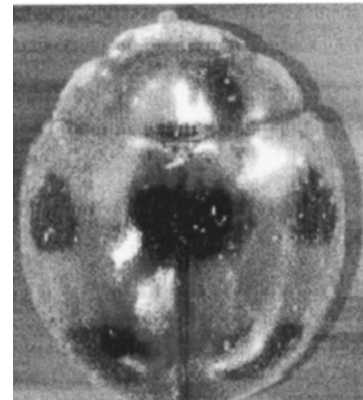
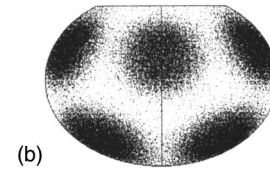
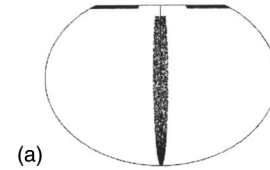


FIG. 6. The geometry of the hard wings of the lady beetle is approximated by a part of a spherical surface, defined in spherical coordinates by  $r = 1$ ,  $\theta_0 < \theta < \pi$ ,  $0 < \varphi < \pi$ .

where  $\Delta \theta = \pi/M$ ,  $\Delta \varphi = \varphi/N$ , and  $\theta$  is evaluated at  $(i - \frac{1}{2})\Delta \theta, (j - \frac{1}{2})\Delta \varphi$ . The zero-flux boundary condition is satisfied by the requirement that the derivatives of  $u$  and  $v$  in the direction normal to the boundary vanish. In the finite difference approximation, they are

$$\begin{aligned} u(i_0 - 1, j) &= u(i_0 + 1, j), \\ u(M + 1, j) &= u(M - 1, j), \\ u(i, j_0 - 1) &= u(i, j_0 + 1), \\ u(i, N + 2 - j_0) &= u(i, N - j_0), \end{aligned} \quad (8)$$

and similar ones for  $v(i, j)$ .



(c)

FIG. 7. (a) Initial and (b) final distributions of  $u$  with diffusion constants  $D_u = 0.0005$ ,  $D_v = 0.035$ , and saturation constant  $\kappa = 0$ . The hard wings are projected on the  $xz$  plane. The final pattern is similar to (c), the pattern of the beetle *Platynaspidium quinquepunctatus*.  $M = 48$ ,  $N = 48$ ,  $i_0 = 9$ , and  $j_0 = 1$ .

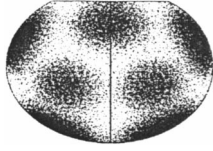


FIG. 8. Final distributions of  $u$  with diffusion constants  $D_u=0.0005$ ,  $D_v=0.025$  and saturation constant  $\kappa=0$ . The pattern is similar to that of the seven-star lady beetle shown in Fig. 1.  $M=48$ ,  $N=48$ ,  $i_0=9$ , and  $j_0=1$ .

## V. RESULTS AND DISCUSSION

With the chosen model, geometry, and numerical method, the calculation to get patterns is not trivial. The necessary condition of Eq. (3) is easy to satisfy but it cannot be used to predict the final patterns of the simulations. The initial condition is crucial for the final pattern. Since there is no experimental evidence for the existence of the morphogens, we have no basis to set the initial distributions of the morphogens. We therefore take this freedom to choose the initial distributions of  $u$  and  $v$  arbitrarily. Random distributions are not considered because they lead to different patterns on the two hard wings. A uniform distribution over the surface or a constant value assigned on part of the boundary of the surface are the simplest reasonable initial setups. For the first example, we take the constants in Eq. (1) as given in Eqs. (4) and (5) and  $D_u=0.0005$ ,  $D_v=70D_u$ ,  $\kappa=0$ . We choose the initial value of  $u$  to be 1.0 on part of the upper boundary and

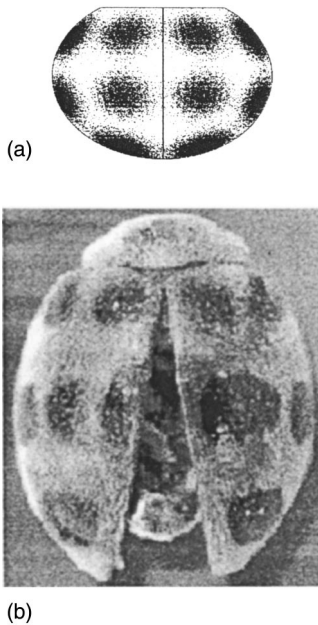
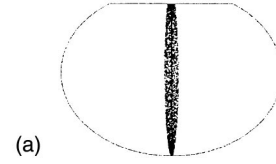


FIG. 9. (a) Final distribution of  $u$  with diffusion constants  $D_u=0.0003$ ,  $D_v=0.04$  and saturation constant  $\kappa=0$ . The pattern is similar to (b), pattern of the beetle *Epilachna crassimala* common in Taiwan.  $M=48$ ,  $N=48$ ,  $i_0=9$ , and  $j_0=1$ .



(a)



(b)



(c)

FIG. 10. (a) Initial and (b) final distributions of  $u$  with diffusion constants  $D_u=0.000028$ ,  $D_v=0.000168$  and saturation constant  $\kappa=0.35$ . The final pattern is similar to (c), pattern of the beetle *Macroilleis hauseri*.  $M=72$ ,  $N=72$ ,  $i_0=19$ , and  $j_0=13$ .

the central band between the two wings as shown in Fig. 7(a), and zero elsewhere. Notice that the central upper region is also set to zero initially. This is crucial in our calculations for spot patterns to have various expected forms. The value of  $v$  is set to 1.0 initially everywhere. Take  $\Delta t=0.001$  for the time step. The distribution of  $u$  finally ( $t=1500$ ) settles down to a pattern of five spots as shown in Fig. 7(b). This is the pattern of the lady beetle *Platynaspidius quinquepunctatus* native to Taiwan [8]. One of the popular species of lady beetles, *Coccinella septempunctata*, called the seven-star beetle in Chinese, has bright red elytra with seven black spots, arranged as 1/2, 2, 1 on each wing (see Fig. 1). The seven-star pattern can be obtained by choosing the diffusion constants to be  $D_u=0.0005$ , and  $D_v=0.025$  with the same initial distribution described above. The resultant pattern from our calculation is plotted in Fig. 8. Another species *Epilachna crassimala* that is also common in Taiwan has ten black spots on the red elytra (Fig. 9). This pattern can be obtained using our model with diffusion coefficients chosen to be  $D_u=0.0003$ ,  $D_v=0.04$ ,  $\kappa=0$ , and the initial distribution of  $u$  on the boundary shown in Fig. 7(a).

To obtain a stripe pattern as in the species *Macroilleis hauseri* shown in Fig. 10(c), we have to adjust the saturation constant to a nonzero value. Choosing  $D_u=0.000028$ ,  $D_v=0.000168$ ,  $\kappa=0.35$ , and an initial distribution of  $u$  as in Fig. 10(a), we obtain the pattern Fig. 10(b), which is indeed

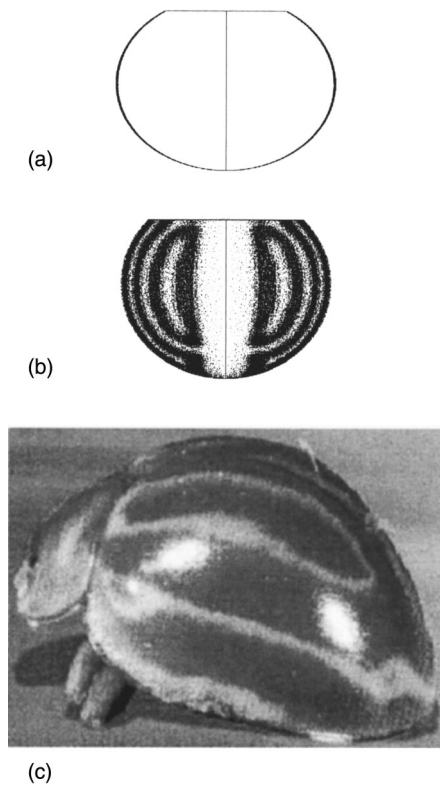


FIG. 11. (a) Initial and (b) final distributions of  $u$  with diffusion constants  $D_u=0.000\ 026$ ,  $D_v=0.000\ 182$  and saturation constant  $\kappa=0.45$ . Additional constant production term for  $u$ ,  $\sigma_u=0.0019$ , is added to Eq. (2) and the central line that separates the two wings is considered as a sink. The final pattern is similar to (c), pattern of the beetle *Bothrocalvia albolineata*.  $M=72$ ,  $N=72$ ,  $i_0=19$ , and  $j_0=6$ .

very similar to the real one. With initial distribution of  $u$  along the upper boundary of the hard wings, the calculation leads to stripe patterns in the  $\varphi$  direction. We can also carefully adjust the diffusion coefficients and saturation constant

such that neither the spot nor stripe pattern is complete dominant. That is, a pattern that is a mixture of spots and stripes is possible.

The pattern of the species *Bothrocalvia albolineata* shown in Fig. 11(c) has a loop on each side of the hard wings. It turns out that it is difficult, if not impossible, to generate this pattern using the no-flux boundary condition. In order to obtain this pattern, we introduce a constant production term for  $u$ ,  $\sigma_u$ , and consider the central line that separates the two wings as a sink for morphogens. That is, the distributions of  $u$  and  $v$  are set to zero on the central line at any time during the process of diffusion. Choosing  $D_u=0.000\ 026$ ,  $D_v=0.000\ 182$ ,  $\kappa=0.45$ , and  $\sigma_u=0.0019$ , and initial distribution of  $u$  as in Fig. 11(a), we obtain the final pattern shown in Fig. 11(b), which is similar to the target pattern, Fig. 11(c).

## VI. CONCLUSION

We have applied a specific type of Turing model to simulate the formation of the patterns on lady beetles' hard wings. The diffusion equations of two interacting morphogens are solved numerically on a surface of constant curvature. Several common lady beetle patterns, such as spots, stripes, and loops, can be obtained by choosing appropriate diffusion coefficients and simple initial distributions of the morphogens. Our calculation offers one more successful example supporting the reaction-diffusion dynamic process as a quite general mechanism in generating biological patterns. Furthermore, we found that the geometry of the organism is essential in reproducing the patterns on it. A more careful study of the effects of various geometries is currently under way.

## ACKNOWLEDGMENT

This work is supported partially by the National Science Council of Republic of China under Grant No. NSC 90-2112-M-005-002.

- 
- [1] A. M. Turing, *Philos. Trans. R. Soc. London, Ser. B* **237**, 37 (1952).  
 [2] H. Meinhardt and M. Klinger, *J. Theor. Biol.* **126**, 63 (1987); J. D. Murray, *ibid.* **88**, 161 (1981); S. Kondo and R. Asai, *Nature (London)* **376**, 765 (1995); H. Meinhardt, *ibid.* **376**, 722 (1995); T. Hofer and P. K. Maini, *ibid.* **380**, 678 (1996).  
 [3] A. T. Koch and H. Meinhardt, *Rev. Mod. Phys.* **66**, 1481 (1994).  
 [4] J. D. Murray, *Mathematical Biology* (Springer, Berlin, 1990).  
 [5] C. Varea, J. L. Aragon, and R. A. Barrio, *Phys. Rev. E* **60**, 4588 (1999).  
 [6] A. Gierer and H. Meinhardt, *Kybernetik* **12**, 30 (1972).  
 [7] R. A. Barrio, C. Varea, J. L. Aragon, and P. K. Maini, *Bull. Math. Biol.* **61**, 483 (1999). A more careful analysis of the curvature effect on the patterns is currently under investigation.  
 [8] G. Y. Yu and H. Y. Wang, *Guidebook to Lady Beetles of Taiwan* (Su-Hsing Publishing, Taiwan, 1999).